

Role of Complex Formation in the Polymerization Kinetics of Modified Epoxy–Amine Systems

Steven Swier,[†] Guy Van Assche, Wendy Vuchelen,[‡] and Bruno Van Mele*

Faculty of Applied Sciences, Department of Physical Chemistry and Polymer Science–FYSC (TW), Vrije Universiteit Brussel–VUB, Pleinlaan 2, B-1050 Brussels, Belgium

Received October 26, 2004; Revised Manuscript Received December 22, 2004

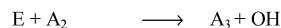
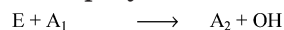
ABSTRACT: The linearly polymerizing diglycidyl ether of bisphenol A (DGEBA) + aniline modified with the low- T_g poly(ethylene glycol) (PEG) is used as a model system to study the importance of complex formation on the cure kinetics of multicomponent epoxy–amines. This system is miscible over the entire conversion range and can be studied without interference of diffusion limitations. A mechanistic model, based on the reaction of amine functionalities with epoxy–hydroxyl complexes, is extended to include physical interactions with PEG. Water and hydroxyl end groups present in the modifier act as catalysts alongside the autocatalysis caused by hydroxyl groups formed. Ether groups of PEG, on the other hand, suppress the reaction rate by forming nonreactive complexes with hydroxyl groups. Accurate reaction rate prediction is achieved of the effect of temperatures from 75 to 130 °C, amine/epoxy molar ratios from 0.6 to 1.4, PEG contents from 9 to 33 wt %, and molecular weights from 400 to 20 000 g mol⁻¹. In addition to the heat flow from modulated temperature DSC (MTDSC), corresponding to the global epoxy conversion rate, the heat capacity signal, containing mechanistic information, can be predicted. The results confirm the importance of complex formation during the polymerization of multicomponent epoxy–amines.

1. Introduction

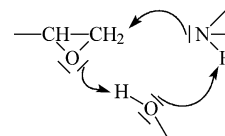
Epoxy resins are a class of thermosetting polymers with high mechanical strength and modulus and good heat and solvent resistance. Applications include structural materials for the aerospace industry and resins for encapsulating electronic components. The demand for tailor-made and application-specific design has initiated interest in multicomponent epoxy systems, for example, to achieve materials with improved impact resistance.^{1,2} Typically, a homogeneous three-component reactive mixture, consisting of epoxy resin, amine hardener, and polymeric modifier, phase separates into a desired heterogeneous morphology due to the unfavorable entropic contribution of the growing epoxy chain (reaction-induced phase separation or RIPS).² While most modifiers result in morphologies in the micrometer range, recent interest in nanostructured thermosets has initiated research in amphiphilic block copolymers as epoxy modifiers.^{3–6}

A wide variety of composite epoxy–amine systems were studied and sometimes with conflicting results. Adding poly(ether imide) to DGEBA-based epoxy–amines was reported to cause just a dilution effect on the reaction rate,^{7,8} while an additional catalytic effect of the tertiary nitrogen atom⁹ was also reported. Poly(methyl methacrylate) (PMMA) shows no interaction with DGEBA¹⁰ but a strong interaction with methylenedianiline (MDA).¹¹ Deviations from an autocatalytic behavior were also found.¹² The reaction kinetics was described mostly with empirical models. Empirical rate laws express the conversion rate in relation to the global

Scheme 1. Epoxy–Amine Reactions



Scheme 2. (Auto)catalysis Due to Complex Formation



conversion of epoxide groups and have proven successful in predicting the effect of reaction temperature on reaction rate.^{13–16} Extensions to semiempirical approaches are needed to include the effect of mixture composition.^{17,18} However, these models are not designed to incorporate differences in epoxy–amine chemistry and possible physical or chemical interactions with additives. This stresses the need for a generalized, mechanistic kinetic model. To select cure schedules for multicomponent epoxy resins, the mechanistic reaction kinetics model is required not only to include the effect of reaction temperature and time but also to incorporate parameters like the three-component composition and specific epoxy/amine/modifier interactions.

In principle, the epoxy–amine polymerization is based on the consecutive epoxy (E)/primary amine (A₁) and epoxy/secondary amine (A₂) reactions (Scheme 1),^{19,20} where A₃ is the tertiary amine and OH the hydroxyl group formed during the reaction. The hydroxyl groups accelerate the epoxy–amine reaction, resulting in the typical autocatalytic behavior. The basis for this acceleration is a termolecular epoxy/amine/hydroxyl complex (Scheme 2).^{21–23} Other complexes arising from hydrogen-bonding interactions between OH, A₁, and the ether group of the epoxy (Et) also have to be considered.^{19,24} On the basis of the conceivable formation of additional complexes, a detailed reaction mechanism was proposed incorporating the effect of interactions

[†] Present address: University of Connecticut, Institute of Materials Science, Polymer Science Program, 97 North Eagleville Rd., Storrs, CT 06269-3136.

[‡] Present address: Total refinery Antwerp NV, Process Engineering & Technical Support, Haven 447-Scheldelaan 16, B-2030 Antwerp, Belgium.

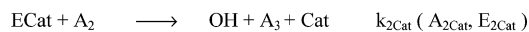
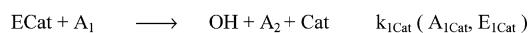
* Corresponding author: e-mail bvmele@vub.ac.be, tel +32-2-6293276, fax +32-2-6293278.

Scheme 3. Detailed Reaction Mechanism for Polymerization of Modified Epoxy–Amine Systems

reactive complexes:



primary and secondary amine–epoxy reaction:



non-reactive complexes:



with the additives on the reaction kinetics (Scheme 3),²⁵ where Cat is either A_1 , primary amine; OH, the hydroxyl groups formed during the reaction; or OH_i , the hydroxyl groups initially present in the reactive mixture (impurities like water or hydroxyl end groups present in the modifier); $\text{Et}_{(\text{mod})}$ designates ether groups commonly present in polymeric modifiers; ECat is an equilibrium complex (termed *reactive complex*) that can further react with A_1 or A_2 in the primary and secondary amine–epoxy reaction, respectively. Notations for the equilibrium constant (K) and reaction rate constants (k) with their respective activation energies (E) and preexponential factors (A) are also given. While the reactive complexes facilitate the reaction causing an acceleration, the *nonreactive* complexes will reduce the concentration of other reactive species and therefore retard the reaction.²³

Scheme 3 was established using a wide range of unmodified epoxy–amine systems using modulated temperature DSC (MTDSC) as the analytical tool: the modeling for a phenyl glycidyl ether (PGE) + aniline²³ model system was extended to the linearly polymerizing diglycidyl ether of bisphenol A (DGEBA) + aniline²⁶ and the network-forming DGEBA + MDA.²⁷ No side reactions like etherification or homopolymerization occur for these systems. Although some recent DSC studies also used a mechanistic approach to the epoxy–amine reaction kinetics,^{28–31} the effect of polymeric additives was not considered. Moreover, MTDSC has the added ability to follow the global conversion rate in the nonreversing heat flow simultaneously with the mechanistic information gathered from the heat capacity signal.³² Possible interference with diffusion-controlled reaction can also be detected as vitrification effects in this sensitive heat capacity signal.^{27,33–35} Note that vitrification of a high- T_g modifier-rich phase can also result in diffusion-controlled reaction and trap some unreacted epoxy–amine molecules.^{34,36–39}

To predict the effect of adding polymeric modifiers like poly(ether sulfone) (PES) and poly(ethylene oxide)-*block*-poly(propylene oxide)-*block*-poly(ethylene oxide) (termed *triblock*), the complexes containing $\text{Et}_{(\text{mod})}$ and OH_i were needed (see Scheme 3).²⁵ In this way, the effect of modifier content on the reaction rate can be predicted. In contrast, from FT-IR spectroscopy no physical or chemical interaction was found between PES and the epoxy–amine.^{40,41} A recent study on the solubility of PES in DGEBA, however, indicates a lower critical solution temperature (LCST) phase behavior, mostly

attributed to specific interactions.⁴² The addition of a tetrafunctional epoxy increased the miscibility window, while the presence of an amine decreased the miscibility, again indicative of the importance of specific epoxy/PES interactions.⁴² Predicting physical interactions in ternary epoxy/amine/modifier systems is therefore crucial to unravel the interplay between thermodynamics, reaction rate, and rate of phase separation during RIPS. The higher concentration of ether groups in the triblock modifier, for example, suppresses autocatalysis to a greater extent than in the case of the PES modifier.²⁵ On the other hand, the low T_g of the triblock modifier ($-70\text{ }^\circ\text{C}$) in comparison to that of PES ($223\text{ }^\circ\text{C}$) does result in a larger extent of phase separation beyond the onset of RIPS.³⁵

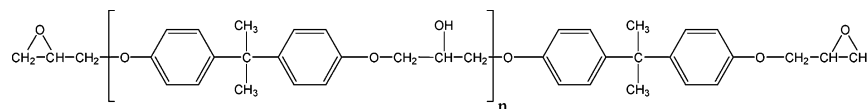
From the onset of RIPS, reactions take place simultaneously in different, interchanging phases. Enrichment of one of the coexisting phases in the epoxy–amine species is responsible for the sudden rate increase typically detected in these systems.^{25,35,36,43,44} This was successfully predicted for the triblock-modified epoxy system.²⁵ The importance of physical interactions also affects the reaction advancement and morphology development in this region. Enrichment of the modifier-rich phase in the more compatible epoxy, for example, resulted in a reaction rate increase in TGDDM + DDS/PEI⁴⁵ and a higher probability of side reactions in TGAP + DDS/PSU.⁴⁶

In this work, the role of complex formation in the cure kinetics of modified epoxy–amine systems will be further elaborated. A model system will be considered based on DGEBA and aniline as the reactive components, modified with the low- T_g polymeric modifier poly(ethylene glycol) (PEG). This modifier is miscible throughout the polymerization^{3,47,48} and can be studied without interference of vitrification. A change in the molecular weight of PEG will test the predictive capability of the mechanistic model for changes in the ether and hydroxyl end group concentration. Moreover, studying the epoxy/amine/modifier interactions independently will impose more restrictions on the equilibrium complexes containing $\text{Et}_{(\text{mod})}$ and OH_i (Scheme 3).

2. Experimental Section

2.1. Techniques. The number-average molecular weights and the molecular weight distributions were determined using a Waters 2690 Alliance gel permeation chromatograph (GPC) equipped with two Styragel HR 5E columns, a Waters 410 differential refractometer, and a Viscotek T50A differential viscometer. The eluent used was tetrahydrofuran (THF). Absolute molecular weights were calculated by performing a universal calibration using polystyrene standards. Thermogravimetric analysis was performed on a Hi-Res Modulated TGA 2950 from TA Instruments. Helium with a flow rate of 50 mL min^{-1} was used as a purge gas, and the Curie point of nickel, alumel, and perkalloy were used for temperature calibration.

Polymerization experiments were performed on a TA Instruments 2920 DSC with MDSC option and a refrigerated cooling system (RCS). Helium was used as a purge gas (25 mL min^{-1}). Indium and cyclohexane were used for temperature calibration. The former was also used for enthalpy calibration. Heat capacity calibration was performed with a PMMA standard (supplied by Acros)⁴⁹ using the (large) heat capacity difference between two temperatures, one above and one below the glass transition temperature of PMMA. In this way, the change of the heat capacity can be calibrated. This is important to adequately detect the change in heat capacity attributed to the epoxy–amine reaction (reaction heat capacity: $\Delta_r C_p$). Polymerization was performed in hermetic aluminum pans (TA

Scheme 4. Diglycidyl Ether of Bisphenol A or DGEBA (Epon Resin 825: $n \rightarrow 0$)Table 1. Specifications of PEG and Related Initial Concentrations for DGEBA + Aniline ($r = 1/\text{PEG}$)

M_n , ^a g/mol	M_n , ^b g/mol	wt % H ₂ O ^d	9 wt % PEG			33 wt % PEG		
			[OH] _(mod) , ^c mol/kg	[H ₂ O], ^e mol/kg	[Et] _(mod) , ^f mol/kg	[OH] _(mod) , ^c mol/kg	[H ₂ O], ^e mol/kg	[Et] _(mod) , ^f mol/kg
400	378	1.42	0.45	0.072	1.87	1.66	0.26	6.83
600	596	0.88	0.30	0.044	1.93	1.11	0.16	7.04
1000	997	0.62	0.18	0.045	1.98	0.66	0.16	7.21
2000	2190	0.25	0.09	0.013	2.01	0.33	0.046	7.34
4000	4636	0.55	0.046	0.028	2.03	0.17	0.10	7.40
20000	n.a. ^c	0.30	0.009	0.015	2.04	0.033	0.055	7.45

^a As specified by the supplier. ^b As determined from GPC. ^c PEG was not soluble in THF. ^d Amount of water present in PEG as determined from TGA (wt % H₂O against total weight). ^e Concentrations of hydroxyl moieties from PEG end groups [OH]_(mod) and water [H₂O]. ^f Concentration of ether functionalities from the modifier [Et]_(mod).

Instruments) with sample weights between 5 and 10 mg. Modulation conditions were an amplitude of 1 °C and a 60 s period.

2.2. Materials. The bifunctional epoxy diglycidyl ether of bisphenol A (DGEBA, $f = 2$) was obtained from Shell as the high-purity Epon Resin 825 (Scheme 4). Aniline was obtained from Aldrich ($f = 2$, $M_w = 93 \text{ g mol}^{-1}$, purity = 99%). Both components were used without further purification and mixed in the appropriate quantities at room temperature.

A single molecular structure is reported for Epon Resin 825, while a low molecular weight component is added to reduce the viscosity ($\text{EEW} = 180 \text{ g mol}^{-1}$).⁵⁰ A GPC analysis reveals a small fraction (less than 5%) of a low molecular weight material. No high molecular weight shoulder is detected, confirming that n is close to zero so that the initial hydroxyl concentration is negligible: Since n equal to zero corresponds to an EEW of 170 g mol^{-1} , a small amount of low molecular weight reactive material might be present in Epon 825 ($\text{EEW} = 180 \text{ g mol}^{-1}$). There is no indication that hydroxyl functionalities are present in this component.²⁶ It is assumed in this work that all epoxide functionalities present have the same reactivity.

Poly(ethylene glycol) (PEG), characterized by two hydroxyl end groups, ranging in molecular weight from 400 to 20 000 g mol^{-1} , was obtained from Aldrich and was used without further purification. The ether groups and hydroxyl groups in PEG are involved in complexes in the reaction mechanism (see also Scheme 3). The molecular weight and the moisture content of the different PEGs were checked by using GPC and TGA, respectively (Table 1). The initial hydroxyl concentration [OH]_i was taken as the sum of the concentration of water and the OH end groups calculated from M_n . As can be seen in Table 1, for molecular weights of less than 4000 g mol^{-1} , the concentration of water is small compared to the concentration of hydroxyl end groups. This limits the influence of small variations in the amount of water present in the low molecular weight modifiers.

DGEBA + aniline/PEG mixtures were prepared by first mixing DGEBA and PEG. Subsequently, the hardener aniline was mixed in at room temperature for a few minutes. This procedure avoids any initial reaction prior to the MTDSC experiment. The mixture composition r will be expressed as the molar ratio of amine functionalities NH to epoxide groups. In this definition, r equal to one corresponds to a stoichiometric epoxy–amine mixture.

2.3. Optimization Software for Reaction Kinetics Modeling (FITME). The software package FITME enables simulations and kinetic parameter optimizations. FITME is based on OPTKIN,⁵¹ a program for mechanistic modeling using kinetic and thermodynamic parameter optimization. Multiple experiments can be optimized simultaneously with one parameter set. The integration routine uses a fourth-order semiimplicit Runge–Kutta method. The optimization routine

used is based on a combination of three algorithms for finding the sum of least squares: Newton–Raphson, steepest descent, and Marquardt.

3. Results and Discussion

3.1. Model Development. 3.1.1. Chemically Controlled Homogeneous Reaction. Although a stoichiometric DGEBA + aniline mixture has a glass transition (T_{gfull}) of 95 °C at full conversion and exhibits diffusion-controlled reaction in the later stages (for a reaction temperature $T_{\text{iso}} < 100 \text{ °C}$ ²⁶), the introduction of PEG (T_{gPEG} ca. −67 °C) as a modifier reduces T_{gfull} significantly. The condition that T_{iso} (as low as 75 °C) is higher than T_{gfull} was fulfilled for all mixture compositions and PEG modifiers used in this study. T_{gfull} already drops below 65 °C by adding 9 wt % PEG.

As indicated before, no complications due to phase separation occur in this system.^{3,47,48} The reaction mechanism, as detailed in Scheme 3, can therefore be used to describe the conversion from a reactive ternary mixture to a fully polymerized PEG-modified epoxy in chemically controlled homogeneous reaction conditions.

3.1.2. Optimization Strategy. A sum of least-squares approach is used to optimize the kinetic model detailed in Scheme 3. The experimentally obtained nonreversing heat flow (d_rH/dt) and reaction heat capacity (Δ_rC_p) from MTDSC can be linked to the concentration profiles simulated by the model³²

$$x(t) = \frac{[E]_0 - [E]}{[E]_0}$$

$$\frac{d_rH}{dt} = \frac{dx}{dt} \Delta_rH \quad (1)$$

$$\Delta_rC_p = \Delta_rC_{p,\text{prim}}([A_2] + [A_3]) + \Delta_rC_{p,\text{sec}}[A_3] \quad (2)$$

with $[E]_0$ and $[E]$ the concentration of epoxide groups (in mol kg^{-1}) at time zero and at time t , respectively, and x the epoxy conversion; Δ_rH is the reaction enthalpy (in kJ mol^{-1}); $[A_2]$ and $[A_3]$ are secondary and tertiary amine concentrations (mol kg^{-1}), respectively; the reaction heat capacity Δ_rC_p is in $\text{J kg}^{-1} \text{ K}^{-1}$, and the reaction heat capacity from the primary amine–epoxy ($\Delta_rC_{p,\text{prim}}$) and secondary amine–epoxy ($\Delta_rC_{p,\text{sec}}$) reaction step is in $\text{J mol}^{-1} \text{ K}^{-1}$.

The direct relation between epoxy conversion rate and nonreversing heat flow (eq 1) has been confirmed for PGE + aniline, DGEBA + aniline, and DGEBA + MDA, characterized by the absence of side reactions like etherification and homopolymerization.³² The rate of epoxide conversion dx/dt will be plotted in the figures.

Equation 2 can be obtained by inspection of Scheme 3. Resolved, mechanistic information is available in the heat capacity signal, since the primary and secondary amine-epoxy reaction steps contribute differently to the reaction heat capacity (in $\text{J mol}^{-1} \text{K}^{-1}$):³²

$$\Delta_r C_{p,\text{prim}} = a + 0.018(T_{\text{cure}} - 298.15) - 0.00085(T_{\text{cure}} - 298.15)^2$$

$$\Delta_r C_{p,\text{sec}} = b + 0.35(T_{\text{cure}} - 298.15) - 0.00024(T_{\text{cure}} - 298.15)^2 \quad (3)$$

with $a = 18.0 \text{ J mol}^{-1} \text{K}^{-1}$ and $b = 19.6 \text{ J mol}^{-1} \text{K}^{-1}$ for both DGEBA + aniline²⁶ and DGEBA + MDA,²⁷ with T_{cure} the reaction temperature in K. At 100°C , for example, $\Delta_r C_{p,\text{prim}}$ and $\Delta_r C_{p,\text{sec}}$ are 15 and $45 \text{ J mol}^{-1} \text{K}^{-1}$, respectively.

The reaction thermodynamics of stoichiometric DGEBA + aniline/PEG mixtures for 9–33 wt % PEG and M_n from 400 to $20\,000 \text{ g mol}^{-1}$ indicates that no correction has to be added for specific interactions involving PEG (normalized for mole epoxide): $\Delta_r H = 98 \pm 5 \text{ kJ mol}^{-1}$ and $\Delta_r C_p = 30 \text{ J mol}^{-1} \text{K}^{-1}$. Possible changes in interactions between PEG and the growing epoxy-amine chain are therefore assumed to have a negligible contribution to both the reaction enthalpy and the reaction heat capacity. Therefore, $\Delta_r H$ and the heat capacity parameters of eq 3 were fixed during optimization in this work.

To obtain a reliable set of adjustable parameters, MTDSC experiments on DGEBA + aniline/PEG were optimized for a wide range of conditions: temperatures varying from 95 to 115°C , PEG molecular weights from 400 to 4000 g mol^{-1} , PEG contents ranging from 9 to 29 wt %, and amine-epoxy molar ratios r from 0.8 to 1.4. The concentration range of OH_i and $\text{Et}_{(\text{mod})}$ is given in Table 1. In the simulations, the actual temperature profile needed to reach the isothermal temperature is taken into account.

The kinetic parameters and equilibrium constants for the unmodified DGEBA + aniline system were fixed, and only the parameters specific to the PEG modification were optimized (indicated with an asterisk in Table 2). This is based on the notion that the unmodified system was successfully described for a wide range of reaction temperature and mixture compositions.²⁶ Moreover, this restricts the amount of adjustable parameters to seven, increasing their accuracy. One set of optimized parameters was obtained (Table 2) for all experimental conditions. The simulation of experimental trends with this set will be shown in section 3.3. Using the parameter values obtained for PEG, the model describes the influence of modification with PES equally well as the previous model, in which some parameter values had to be adjusted depending on the modifier used.²⁵

Table 2 indicates that the primary amine-epoxy reaction catalyzed by primary amines ($k_{1\text{AI}}$) is over 1 order of magnitude slower as compared to the one catalyzed by hydroxyl groups ($k_{1\text{OH}}$), in agreement with other studies.^{23,24,52,53} A reactivity ratio for the OH-catalyzed reaction ($k_{2\text{OH}}/k_{1\text{OH}} = 0.43$) close to 0.5 indi-

Table 2. Optimized Parameters for DGEBA + Aniline/PEG^a

kinetic parameters								
primary amine-epoxy reaction								
$E_{1\text{AI}}$	$\log A_{1\text{AI}}$	$k_{1\text{AI}}$	$E_{1\text{OH}}$	$\log A_{1\text{OH}}$	$k_{1\text{OH}}$	$E_{1\text{OHi}}$	$\log A_{1\text{OHi}}$	$k_{1\text{OHi}}$
79.6	7.5	2.3	48.0	4.4	47	56.5*	4.9*	10
secondary amine-epoxy reaction								
	$E_{2\text{OH}}$	$\log A_{2\text{OH}}$	$k_{2\text{OH}}$	$E_{2\text{OHi}}$	$\log A_{2\text{OHi}}$	$k_{2\text{OHi}}$		
	48.4	4.1	20	54.4*	4.3*	5		
equilibrium constants								
reactive complexes			non-reactive complexes					
K_{EAI}	K_{EOH}	K_{EOHi}	K_{A1OH}	K_{EtOH}	K_{E1AI}	$K_{\text{Et(mod)OH}}$	$K_{\text{Et(mod)OHi}}$	
0.18	0.20	0.19*	0.50	0.55	0.18	0.48*	0.21*	

^a Optimized parameters are designated with an asterisk; other parameters were taken from the optimized set for DGEBA + aniline.²⁶ Reaction rate constants (k_i) are given at 100°C in $10^{-4} \text{ kg mol}^{-1} \text{s}^{-1}$. Activation energies (E) are in kJ mol^{-1} . Preexponential Factors (A) are in $\text{kg mol}^{-1} \text{s}^{-1}$. Equilibrium constants are in kg mol^{-1} .

cates that a negligible substitution effect is present in the DGEBA + aniline system, also observed elsewhere.^{26,54} Note that the parameters of the OH_i -catalyzed reaction are sensitive to the (less reliable) initial reaction rate. Interpretation of these parameters would therefore be tentative. Nevertheless, the ratio $k_{2\text{OHi}}/k_{1\text{OHi}} = 0.5$ is in agreement with a negligible substitution effect. The higher equilibrium constant of the $\text{Et}_{(\text{mod})}\text{OH}$ and EtOH complexes in comparison to the $\text{Et}_{(\text{mod})}\text{OHi}$ might indicate that the latter pair exhibits weaker interactions. The small difference between the $\text{Et}_{(\text{mod})}\text{OH}$ and EtOH equilibrium rate constants (Table 2) and the fact that the same parameters can be used for a PES-modified system point out that one could group these two equilibrium constants and treat them as one parameter. However, to avoid modifying the original model for the unmodified DGEBA + aniline system, the equilibrium constants of the complex formation of $\text{Et}_{(\text{mod})}\text{OH}$ were treated independently, keeping the equilibrium constant of the formation of the EtOH complex fixed. The importance of these nonreactive complexes is well-known^{19,24} and was illustrated by simulation for the model system PGE + aniline.²³ Simulations for the PEG-modified system in section 3.3 will serve as further clarification. Although the equilibrium constants are within the range found in the literature,^{19,24} further research on other epoxy-amine additives has to be done to impose more restrictions and increase the amount of independent variables. A valuable extension of the current approach is the implementation of temperature-dependent equilibrium constants, which is part of future work.

3.2. Contribution from Different Reaction Steps.

The additional steps in Scheme 3 (indicated with an asterisk in Table 2), needed to account for the effect of the PEG modifier on the epoxy conversion rate, can be understood by simulating them separately (Figure 1). The simulation for the unmodified DGEBA + aniline system is shown for reference in Figure 1a; details in ref 26). When the modifier is assumed to be inert, therefore only causing a dilution of reactive epoxy-amine groups, the reaction rate of the PEG-modified system is described poorly (Figure 1b). The formation of $\text{Et}_{(\text{mod})}\text{OH}$ complexes results in a decrease of the EOH

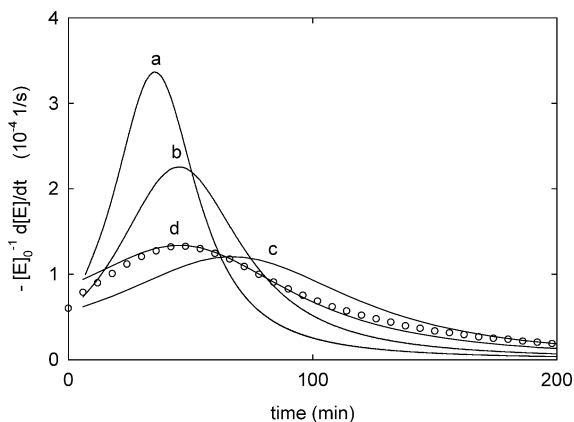


Figure 1. Simulation of the different contributions to the epoxy conversion rate for the reaction of DGEBA + aniline/29 wt % PEG ($M_n = 2.000 \text{ g mol}^{-1}$) at 115°C : unmodified DGEBA + aniline (a), only dilution of reactive groups (b), introduction of $\text{Et}_{(\text{mod})}\text{OH}$ complexes (c) and OH_i from modifier (d); experimental points (\circ).

concentration, responsible for the suppressed catalytic behavior (Figure 1c). Finally, accounting for the OH_i from PEG (end groups and water present in it) is crucial to simulate the experiment correctly (Figure 1d).

For unmodified epoxy systems, in the absence of hydroxyl impurities, the initial reaction rate was found to depend in second order on the primary amine concentration,^{23,26} indicating that the primary amine itself forms a complex with the epoxy (similar to the EOH complex shown in Scheme 2). When the PEG modifier is added, however, impurities like water or hydroxyl end groups will also act as catalysts (Scheme 3). This can be confirmed by calculating the initial reaction rate from inspection of Scheme 3:

$$\begin{aligned} v_0 &= -\frac{d[\text{E}]}{dt}\bigg|_0 = k_{1\text{A1}}[\text{EA}]_0[\text{A}]_0 + k_{1\text{OH}_i}[\text{EOH}_i]_0[\text{A}]_0 \\ &= k_{1\text{A1}}K_{\text{EA1}}[\text{E}]_0[\text{A}]_0^2 + k_{1\text{OH}_i}K_{\text{EOH}_i}[\text{E}]_0[\text{OH}_i]_0[\text{A}]_0 \end{aligned} \quad (4)$$

Equation 1 can be used to obtain this rate from the heat flow at $t = 0$, $(d_t H/dt)_0$:

$$-\frac{d[\text{E}]}{dt}\bigg|_0 \frac{1}{[\text{E}]_0} = \frac{dx}{dt}\bigg|_0 = \frac{d_t H}{dt}\bigg|_0 \frac{1}{\Delta_r H} \quad (5)$$

The normalized initial reaction rate ($v_0/[\text{E}]_0$), obtained from simulation, has been plotted as a function of the initial primary amine concentration at 100°C in Figure 2 (log–log scale). The order in A_1 is lower than two (1.6), confirming the importance of the additional catalytic reaction (eq 4). It should be noted that the order in A_1 is found to be 2.0 at 100°C for the unmodified DGEBA–aniline system.²⁶

The hydroxyl end groups and water present in PEG (OH_i) can also catalyze the secondary amine–epoxy reaction ($k_{2\text{OH}_i}$ in Table 2). The ratio of reaction rates, $v_{2\text{OH}_i}/v_{2\text{OH}}$, is plotted as a function of epoxy conversion in Figure 3 for a stoichiometric DGEBA + aniline mixture modified with 15 wt % PEG ($M_w = 400 \text{ g mol}^{-1}$). Catalysis with the OH_i groups is predominant up to a conversion of 10%, indicating its importance in the mechanism. Autocatalysis with the formed OH groups becomes important from this point on. Catalysis with

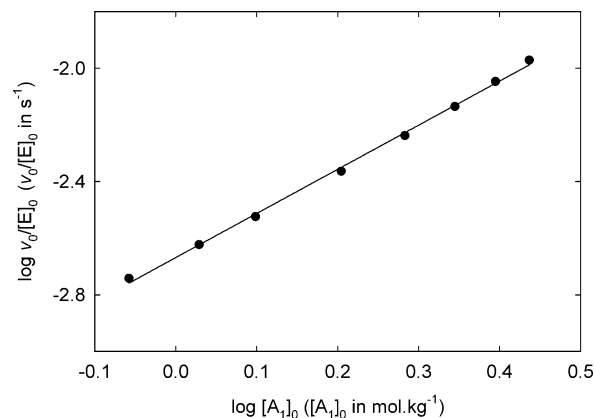


Figure 2. Normalized initial reaction rate ($v_0/[\text{E}]_0$ in s^{-1}) at 100°C as calculated from the nonreversing heat flow signal as a function of the initial concentration (in mol kg^{-1}) of primary amine groups (\bullet) (log–log scale): best fit gives a reaction order of 1.6.

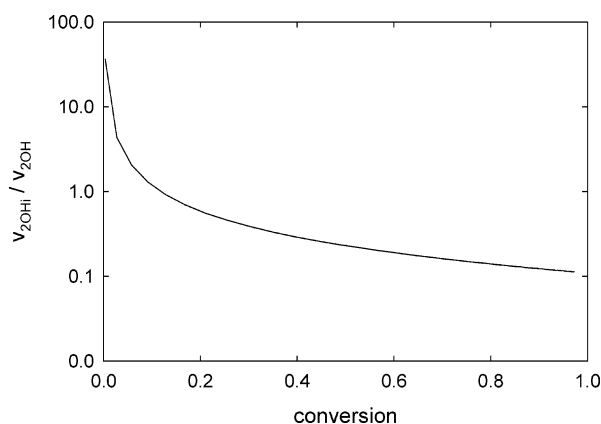


Figure 3. Ratio of reaction rates of OH_i -catalyzed ($v_{2\text{OH}_i}$) to OH -catalyzed ($v_{2\text{OH}}$) consumption of secondary amines at 100°C as a function of epoxy conversion in DGEBA + aniline ($r = 1$) for 15 wt % PEG ($M_n = 400 \text{ g mol}^{-1}$).

OH_i groups is less important for the PES ($20\,000 \text{ g mol}^{-1}$) system and was therefore neglected previously.²⁵

3.3. Simulation of Experimental Trends in PEG-Modified DGEBA + Aniline. The simulation flexibility of the mechanistic model in Scheme 3 was validated by predicting effects like the epoxy–amine/PEG composition, the molecular weight of PEG, and the reaction temperature/time. Stoichiometric epoxy–amine compositions will be used in sections 3.3.1 and 3.3.2, while the epoxy–amine composition will be altered in section 3.3.3. It has to be stressed that one optimized set of parameters (Table 2) will be used for all simulations and that the conditions of several of the simulated experiments are outside the ranges used for optimization.

3.3.1. Molecular Weight and Weight Fraction of Poly(ethylene glycol). As indicated in the discussion of Figure 1, the addition of PEG reduces the reaction rate by dilution and interaction with the ether groups. The initial reaction stages are strongly influenced by OH_i catalysis. For the same wt % of PEG, using a low molecular weight PEG results in a high OH_i concentration, which increases the initial reaction rate (see Table 1 and Figure 4). Moreover, a change in the molecular weight of PEG alters the initial hydroxyl (OH_i)/ether ($\text{Et}_{(\text{mod})} + \text{Et}$) ratio and hence the balance between the opposing effects of reactive and nonreactive complexes. As seen in Figure 4, not only the initial rate (v_i)

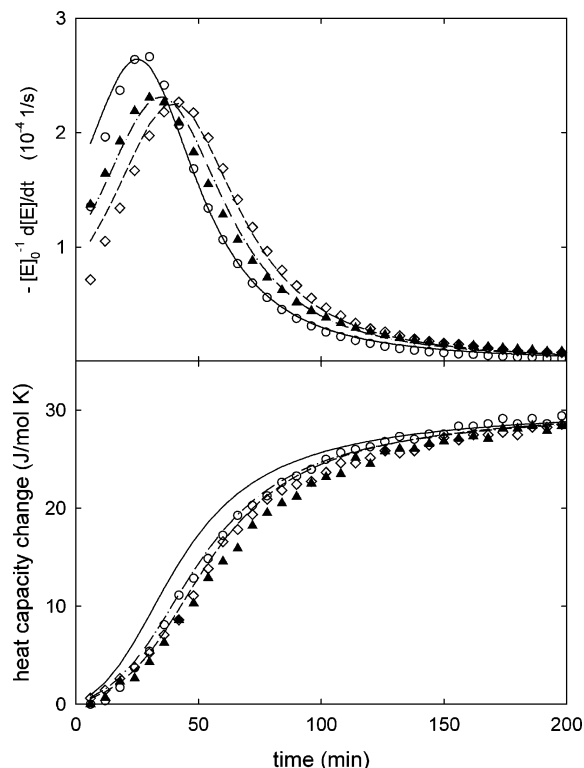


Figure 4. Rate of epoxide conversion (dx/dt) and change in heat capacity for DGEBA + aniline ($r = 1$)/13 wt % PEG polymerized at 115 °C as a function of PEG M_n ; simulations using the parameter set of Table 2 (lines), experiments (symbols): $M_n = 400$ g mol $^{-1}$ (\circ , solid line), $M_n = 1000$ g mol $^{-1}$ (\blacktriangle , dash-dot line), and $M_n = 4000$ g mol $^{-1}$ (\diamond , dashed line).

decreases, but also the maximum rate (v_{\max}) is delayed and the autocatalytic effect (calculated as v_{\max}/v_i) is stronger when the molecular weight increases: v_{\max}/v_i changes from 3 ($M_n = 400$ g mol $^{-1}$) to 5 ($M_n = 4000$ g mol $^{-1}$). This effect is caused by the larger relative increase of the total hydroxyl concentration, $\text{OH} + \text{OH}_i$. Figure 4 also shows the simulation of the heat capacity signal. Although the simulations are slightly higher than the experimental results, the molecular weight effect of the PEG modifier is well predicted in terms of the initial OH_i concentration, the hydroxyl/ether ratio, and the relative increase of the total hydroxyl concentration. Note that the parameters for the heat capacity (eqs 2 and 3) were not optimized and correspond to the ones obtained for the unmodified epoxy-amine system.

A clear drop in the overall rate is seen in Figure 5 when the modifier fraction is increased. This is again due to the combination of dilution and the formation of a nonreactive complex. The interplay between these effects and the opposing increase in OH_i concentration is well predicted. Although the PEG concentration is varied by a factor of 2.5, the variation of the initial rate is clearly smaller due to this competition between reactive (OH_i effect) and nonreactive ($\text{Et}_{(\text{mod})}$ effect) complexes.

3.3.2. Reaction Temperature. Raising the reaction temperature from 75 to 130 °C increases the overall reaction rate more than an order of magnitude, as is well predicted by the model (Figure 6). This confirms the validity of the activation energies in Table 2. Accurate prediction of the temperature effect for these composite epoxy-amines is important for cure schedule selection in processing. The increase in reaction heat capacity $\Delta_r C_p$ with temperature, as calculated from eqs

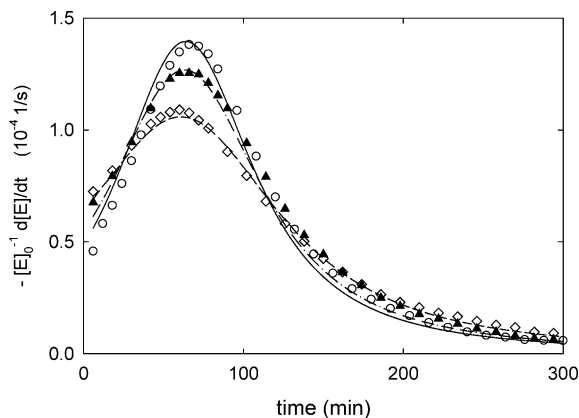


Figure 5. Rate of epoxide conversion (dx/dt) for DGEBA + aniline ($r = 1$)/PEG ($M_n = 600$ g mol $^{-1}$) polymerized at 100 °C as a function of wt % PEG; simulations using the parameter set of Table 2 (lines), experiments (symbols): 9 wt % (\circ , solid line), 13 wt % (\blacktriangle , dash-dot line), and 23 wt % PEG (\diamond , dashed line).

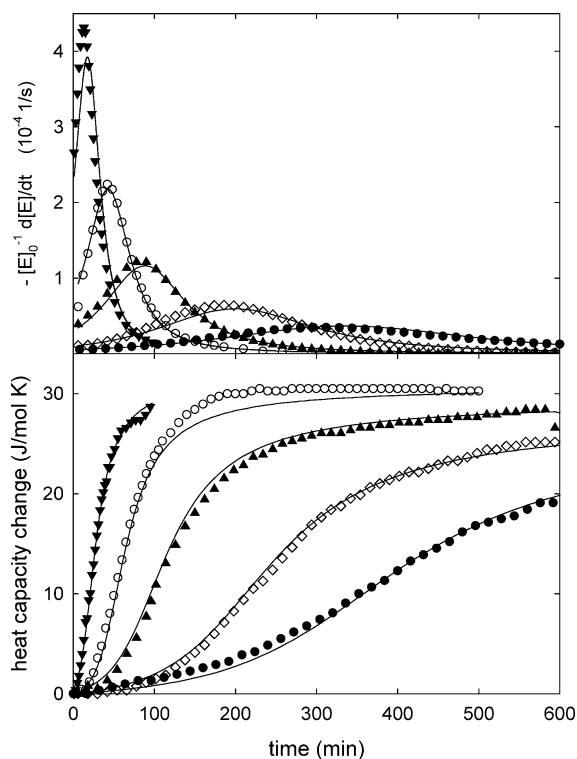


Figure 6. Rate of epoxide conversion (dx/dt) and heat capacity change for DGEBA + aniline ($r = 1$)/13 wt % PEG ($M_n = 20\,000$ g mol $^{-1}$) polymerized at different temperatures; simulations using the parameter set of Table 2 (lines), experiments (symbols): 130 (\blacktriangledown), 115 (\circ), 100 (\blacktriangle), 85 (\diamond), and 75 °C (\bullet).

2 and 3,³² corresponds to the experimental trend. Note that the heat capacity parameters were previously optimized for the unmodified DGEBA + aniline in a similar temperature range (60–110 °C).²⁶ The lower reaction rate of the PEG-modified system allows for the extension to higher temperatures.

A further extension of the temperature range far beyond the 95–115 °C range used for the optimization is achieved in nonisothermal experiments with different heating rates (Figure 7). Side reactions like homopolymerization and etherification were not found for the unmodified DGEBA + aniline system.²⁶ These reactions do not seem to be promoted by the presence of PEG, as evidenced by the absence of an additional exothermic

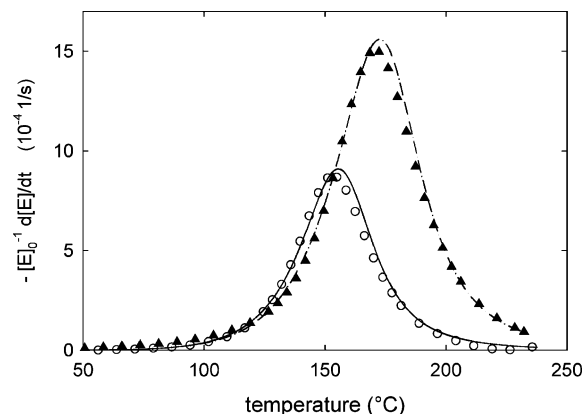


Figure 7. Rate of epoxide conversion (dx/dt) for DGEBA + aniline ($r = 1$)/13 wt % PEG ($M_n = 20\,000\text{ g mol}^{-1}$) polymerized in nonisothermal conditions; simulations using the parameter set of Table 2 (lines), experiments (symbols): 2.5 °C/min (○, solid line) and 5 °C/min (▲, dash-dot line).

peak at higher temperatures. However, the occurrence of side reactions in the case of a large excess in epoxide groups cannot be excluded.^{19,55,56} These side reactions might be catalyzed by the OH_i moieties. In that case, and if these experimental conditions are of importance, additional reaction steps are needed in the model. The corresponding model parameters can be optimized by fitting well-chosen supplementary experiments, proving the flexibility of the mechanistic approach.

3.3.3. Epoxy–Amine Composition. The increase in reaction rate for an excess in amine groups, correctly simulated in Figure 8, can be understood from their catalytic effect. This results in a higher reaction order of amine groups in comparison to epoxide groups (calculated for the initial reaction rate in eq 4). The addition of PEG introduces the competing OH_i catalyst, altering this balance slightly (see also Figure 2).

The lower value of $\Delta_r C_{p,\text{prim}}$ in comparison to $\Delta_r C_{p,\text{sec}}$ at 100 °C (eq 3) results in a lower $\Delta_r C_p$, calculated per mole of the minority component, for an excess of amine (compare $r = 0.8$ with $r = 1.4$ in Figure 8). For an excess of epoxide groups or stoichiometric conditions, $\Delta_r C_p$ tends to the same maximum value at full conversion of the minority component (compare $r = 0.8$ with $r = 1.0$ in Figure 8). This effect was studied in detail over a wide range of mixture compositions (r from 0.4 to 3.6) for the model system PGE + aniline.³²

4. Conclusions

The importance of complex formation during reaction of multicomponent epoxy–amines can be confirmed by considering a model system based on the linearly polymerizing DGEBA + aniline modified with the low- T_g modifier PEG. By changing the molecular weight and content of this modifier, the impact of the ether group and hydroxyl end group concentration on the reaction rate can be investigated.

The mechanistic model consists of basic amine–epoxy reactions together with reactive and nonreactive complexes. Apart from the dilution of epoxy–amine groups by the modifier, additional steps have to be included to account for the physical interaction with PEG. Hydroxyl end groups and impurities like moisture result in catalysis of the primary amine–epoxy reaction, clearly evidenced by the smaller reaction order in A_1 . In an intermediate conversion range, OH_i catalysis of the secondary amine–epoxy reaction is competitive with

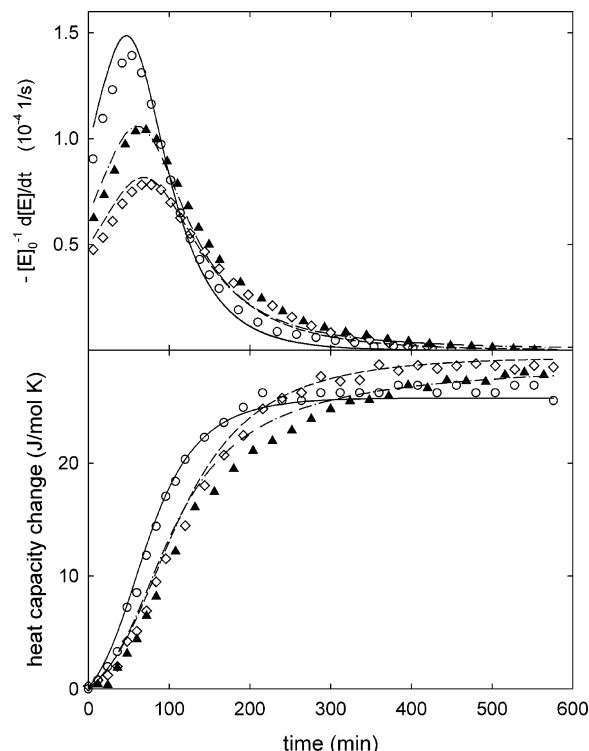


Figure 8. Rate of epoxide conversion (dx/dt) and heat capacity change (per mole of the minority functionality: E for $r \geq 1$, NH for $r < 1$) for DGEBA + aniline/23 wt % PEG ($M_n = 600\text{ g mol}^{-1}$) polymerized at 100 °C; simulations using the parameter set of Table 2 (lines), experiments (symbols): $r = 1.4$ (○, solid line), $r = 1$ (▲, dash-dot line), and $r = 0.8$ (◇, dashed line).

autocatalysis resulting from formed OH groups. The ether groups in PEG suppress catalysis and autocatalysis by trapping OH_i and OH groups, respectively, in nonreactive complexes.

Trends in rate of epoxide conversion (heat flow) and heat capacity from MTDSC experiments can be accurately predicted by using the developed mechanistic approach. The additional parameters were optimized while keeping the parameters associated with the unmodified DGEBA + aniline system unaltered. This reduces the amount of adjustable parameters, increasing their accuracy. Apart from the effect of reaction temperature and time, the effect of epoxy–amine/PEG composition and PEG molecular weight can also be simulated. Close correspondence between simulated and experimental heat capacity evolutions, obtained without changing the $\Delta_r C_p$ parameters, confirms that $\Delta_r C_{p,\text{prim}}$ is smaller than $\Delta_r C_{p,\text{sec}}$ at typical reaction temperatures. Increasing the reaction temperature increases this difference. Currently, the equilibrium constants were kept temperature independent in the modeling. In future work, the temperature dependence will be accounted for.

In contrast to our previous work on modified epoxy–amines, the refined model based on the PEG modifier is able to predict the impact of another polymeric modifier containing ether and hydroxyl groups but differing in structure and thermal properties. This is promising in view of evaluating the effect of new polymeric modifiers and low molecular weight additives used in commercial thermoset applications. Further research is currently considered to extend the mechanistic model beyond the onset of RIPS by incorporating

interdiffusion between coexisting phases in a heterogeneous system.

Acknowledgment. Guy Van Assche is a postdoctoral fellow of the Fund for Scientific Research–Flanders (Belgium).

References and Notes

- Hodgkin, J. H.; Simon, G. P.; Varley, R. J. *Polym. Adv. Technol.* **1998**, *9*, 3–10.
- Williams, R. J. J.; Rozenberg, B. A.; Pascault, J. P. *Adv. Polym. Sci.* **1997**, *128*, 95–156.
- Mijovic, J.; Shen, M. Z.; Sy, J. W.; Mondragon, I. *Macromolecules* **2000**, *33*, 5235–5244.
- Lipic, P. M.; Bates, F. S.; Hillmyer, M. A. *J. Am. Chem. Soc.* **1998**, *120*, 8963–8970.
- Hillmyer, M. A.; Lipic, P. M.; Hajduk, D. A.; Almdal, K.; Bates, F. S. *J. Am. Chem. Soc.* **1997**, *119*, 2749–2750.
- Grubbs, R. B.; Dean, J. M.; Broz, M. E.; Bates, F. S. *Macromolecules* **2000**, *33*, 9522–9534.
- Bonnaud, L.; Pascault, J. P.; Sautereau, H. *Eur. Polym. J.* **2000**, *36*, 1313–1321.
- Bonnet, A.; Pascault, J. P.; Sautereau, H.; Taha, M.; Camberlin, Y. *Macromolecules* **1999**, *32*, 8517–8523.
- Girard-Reydet, E.; Riccardi, C. C.; Sautereau, H.; Pascault, J. P. *Macromolecules* **1995**, *28*, 7599–7607.
- Ritzenthaler, S.; Girard-Reydet, E.; Pascault, J. P. *Polymer* **2000**, *41*, 6375–6386.
- Mondragon, I.; Remiro, P. M.; Martin, M. D.; Valea, A.; Franco, M.; Bellenger, V. *Polym. Int.* **1998**, *47*, 152–158.
- Remiro, P. M.; Riccardi, C. C.; Corcuera, M. A.; Mondragon, I. *J. Appl. Polym. Sci.* **1999**, *74*, 772–780.
- Kamal, M. R. *Polym. Eng. Sci.* **1974**, *14*, 231–239.
- Vyazovkin, S.; Shbirrazzuoli, N. *Macromolecules* **1996**, *29*, 1867–1873.
- Van Assche, G.; Van Hemelrijck, A.; Rahier, H.; Van Mele, B. *Thermochim. Acta* **1996**, *286*, 209–224.
- Van Assche, G.; Swier, S.; Van Mele, B. *Thermochim. Acta* **2002**, *388* (1–2), 327–341.
- Horie, K.; Hiura, H.; Sawada, M.; Mita, I.; Kambe, H. *J. Polym. Sci., Part A: Polym. Chem.* **1970**, *8*, 1357–1372.
- Cole, K. C. *Macromolecules* **1991**, *24*, 3093–3097.
- Rozenberg, B. A. *Adv. Polym. Sci.* **1986**, *75*, 113–165.
- Barton, J. M. *Adv. Polym. Sci.* **1985**, *72*, 111–154.
- Shechter, L.; Wynstra, J.; Kurkij, R. P. *Ind. Eng. Chem.* **1956**, *48*, 94–97.
- Smith, I. R. *Polymer* **1961**, *2*, 95–108.
- Swier, S.; Van Mele, B. *Thermochim. Acta* **2004**, *411*, 149–169.
- Enikolopiyan, N. S. *Pure Appl. Chem.* **1976**, *48*, 317–328.
- Swier, S.; Van Mele, B. *Macromolecules* **2003**, *36*, 4424–4435.
- Swier, S.; Van Assche, G.; Van Mele, B. *J. Appl. Polym. Sci.* **2004**, *91*, 2798–2813.
- Swier, S.; Van Assche, G.; Van Mele, B. *J. Appl. Polym. Sci.* **2004**, *91*, 2814–2833.
- Flammersheim, H. J.; Opfermann, J. R. *Macromol. Mater. Eng.* **2001**, *286*, 143–150.
- Flammersheim, H. J.; Opfermann, J. R. *Thermochim. Acta* **2002**, *388*, 389–400.
- Zvetkov, V. L. *Macromol. Chem. Phys.* **2002**, *203*, 467–476.
- Riccardi, C. C.; Fraga, F.; Dupuy, J.; Williams, R. J. J. *J. Appl. Polym. Sci.* **2001**, *82*, 2319–2325.
- Swier, S.; Van Mele, B. *J. Polym. Sci., Part B: Polym. Phys.* **2003**, *41*, 594–608.
- Van Assche, G.; Van Hemelrijck, A.; Rahier, H.; Van Mele, B. *Thermochim. Acta* **1995**, *268*, 121–142.
- Swier, S.; Van Assche, G.; Van Hemelrijck, A.; Rahier, H.; Verdonck, E.; Van Mele, B. *J. Therm. Anal. Calorim.* **1998**, *54*, 585–604.
- Swier, S.; Van Mele, B. *Polymer* **2003**, *44*, 2689–2699.
- Swier, S.; Van Mele, B. *Polymer* **2003**, *44*, 6789–6806.
- Barral, L.; Cano, J.; Lopez, J.; Lopez-Bueno, I.; Nogueira, P.; Torres, A.; Ramirez, C.; Abad, M. *J. Thermochim. Acta* **2000**, *344*, 127–136.
- Poncet, S.; Boiteux, G.; Pascault, J. P.; Sautereau, H.; Seytre, G.; Rogozinski, J.; Kranbuehl, D. *Polymer* **1999**, *40*, 6811–6820.
- Swier, S.; Van Mele, B. *Thermochim. Acta* **1999**, *330*, 175–187.
- MacKinnon, A. J.; Jenkins, S. D.; McGrail, P. T.; Pethrick, R. A. *Macromolecules* **1992**, *25*, 3492–3499.
- Martinez, I.; Martin, M. D.; Eceiza, A.; Oyanguren, P.; Mondragon, I. *Polymer* **2000**, *41*, 1027–1035.
- Bonnaud, L.; Bonnet, A.; Pascault, J. P.; Sautereau, H.; Riccardi, C. C. *J. Appl. Polym. Sci.* **2002**, *83*, 1385–1396.
- Tran-Cong, Q.; Shibayama, M. *Structure and Properties of Multiphase Polymeric Materials*; Marcel Dekker: New York, 1998.
- Bonnet, A.; Pascault, J. P.; Sautereau, H.; Camberlin, Y. *Macromolecules* **1999**, *32*, 8524–8530.
- Su, C. C.; Woo, E. M. *Polymer* **1995**, *36*, 2883–2894.
- Varley, R. J.; Hodgkin, J. H.; Hawthorne, D. G.; Simon, G. P.; McCulloch, D. *Polymer* **2000**, *41*, 3425–3436.
- Guo, Q. P.; Thomann, R.; Gronski, W.; Thurn-Albrecht, T. *Macromolecules* **2002**, *35*, 3133–3144.
- Zheng, S.; Zhang, N.; Luo, X. *Polymer* **1995**, *36*, 3609–3613.
- Gaur, U.; Wunderlich, B. *J. Phys. Chem. Ref. Data* **1982**, *11*, 313–325.
- Shell. method HC-427-81: Perchloric acid method.
- Huybrechts, G.; Van Assche, G. *Comput. Chem.* **1998**, *22*, 413–417.
- Xu, L.; Fu, J. H.; Schlup, J. R. *J. Am. Chem. Soc.* **1994**, *116*, 2821–2826.
- Flammersheim, H. J. *Thermochim. Acta* **1998**, *310*, 153–159.
- Charlesworth, J. M. *J. Polym. Sci., Part A: Polym. Chem.* **1987**, *25*, 731–734.
- Cole, K. C.; Hechler, J. J.; Noel, D. *Macromolecules* **1991**, *24*, 3098–110.
- Mijovic, J.; Wijaya, J. *Polymer* **1994**, *35*, 2683–2686.

MA047796X